Escherichia coli RNA polymerase-associated SWI/SNF protein RapA: evidence for RNA-directed binding and remodeling activity

Brian A. McKinley and Maxim V. Sukhodolets*

Laboratory of Biochemistry, Department of Chemistry, Lamar University, Beaumont, TX 77710, USA

ABSTRACT

Helicase-like SWI/SNF proteins are present in organisms belonging to distant kingdoms from bacteria to humans, indicating that they perform a very basic and ubiquitous form of nucleic acid management; current studies associate the activity of SWI/SNF proteins with remodeling of DNA and DNA–protein complexes. The bacterial SWI/SNF homolog RapA—an integral part of the *Escherichia coli* RNA polymerase complex—has been implicated in remodeling post-termination DNA–RNA polymerase–RNA ternary complexes (PTC), however its explicit nucleic acid substrates and mechanism remain elusive. Our work presents evidence indicating that RNA is a key substrate of RapA. Specifically, the formation of stable RapA–RNA intermediates in transcription and other, independent lines of evidence presented herein indicate that RapA binds and remodels RNA during transcription. Our results are consistent with RapA promoting RNA release from DNA–RNA polymerase–RNA ternary complexes; this process may be accompanied by the destabilization of non-canonical DNA–RNA complexes (putative DNA–RNA triplexes). Taken together, our data indicate a novel RNA remodeling activity for RapA, a representative of the SWI/SNF protein superfamily.

INTRODUCTION

The SWI/SNF superfamily of proteins contains a large number of representatives, present in many living species from bacteria to humans, which share six characteristic helicase-like motifs (1–3). However, the explicit role of these helicase-like protein subdomains remains undetermined, and none of the proteins of this superfamily described to date has shown helicase activity in conventional *in vitro* helicase assays utilizing duplex nucleic acid substrates. Mutations in SWI/SNF genes have been associated with pediatric cancers of brain and soft tissue (4,5) and leukemia (6); multiple, independent studies indicate that SWI/SNF proteins act as tumor suppressors (7–10). *In vitro*, purified SWI/SNF complexes produce ATP-dependent alterations of the chromatin structure, and these observations eventually led to the idea that SWI/SNF complexes act primarily as chromatin remodeling machines (11–14). In mammals, *Drosophila* and yeast, the multiple individual SWI/SNF polypeptides are present as integral components of large multi-subunit nuclear complexes. The specific roles of individual SWI/SNF polypeptides in eukaryotic SWI/SNF and other nuclear complexes are debated. It has been suggested that the ATP-propelled sliding of SWI/SNF proteins along DNA might enhance nucleosome translocation during transcription and other cellular events that involve DNA (15–18). Existing studies associate the activity of SWI/SNF proteins almost exclusively with remodeling of DNA and histone–DNA complexes, and their primary role *in vivo* is proposed to be global regulation of transcription and gene expression.

In contrast, *Escherichia coli* contains only a single 110-kDa SWI/SNF polypeptide (19,20), which shares homology with its eukaryotic counterparts throughout six characteristic helicase-like subdomains (1–3), suggesting that they share similar basic functions. This homology also makes the *E. coli* SWI/SNF protein RapA (19,21) a particularly attractive target for analysis of the explicit role(s) of SWI/SNF polypeptides. RapA—also referred to as HepA (20)—was identified as a subunit of the *E. coli* RNA polymerase complex (19,22,23). This relatively abundant protein, the copy number of which is roughly comparable to that of the RNA polymerase sigma^{70} subunit, binds preferentially to the core RNA polymerase (with the K_d of the complex being in the nanomolar range, indicating a high degree of specificity of the interaction) at the interface of the alpha and beta-prime RNA polymerase subunits (22). Rigorous study of *rapA* deletion

*To whom correspondence should be addressed. Tel: +1 409 880 7905 (office) +1 409 880 7906 (laboratory); Fax: +1 409 880 8270; Email: msoukhodol@my.lamar.edu

mutation strains has produced no evidence of significant alterations in their rate of growth, mutation rates or UV sensitivity in comparison with *rapA* plus strains under a variety of experimental conditions (22), suggesting that the role of RapA differs from those proposed for eukaryotic SWI/SNF polypeptides. However, *rapA* deletion produces a unique phenotype, rendering bacteria incapable of efficient growth at relatively high salt concentrations in LB agar (23). Analysis of the role of RapA in transcription has indicated its capability for conditional stimulation of the polymerase's transcriptional activity (in a salt concentration-specific fashion, consistent with the *in vivo* effect of the *rapA* deletion mutation) likely via promoting the dissociation of one or more components of the DNA–RNA polymerase–RNA ternary complex (23). However, it remains unclear which component(s) of non-productive post-termination ternary complexes are specifically targeted by RapA; our previous hypotheses—based on studies with eukaryotic SWI/SNF proteins—solely focused on DNA as a substrate of RapA. The question of the explicit nucleic acid- and/or protein substrate specificity of RapA is important, because the function of SWI/SNF motifs V and VI have not been fully explained. Although they are present in all SWI/SNF proteins in addition to helicase-like motifs I–IV, studies of distantly related DEAD/H DNA helicases have suggested that motifs I–IV may be sufficient for translocation along DNA. X-ray structures of the catalytic domain of the RapA homolog from *Sulfolobus solfataricus* (SsoRad54) complexed to DNA have further confirmed DNA binding by a bacterial SWI/SNF protein and indicate that SWI/SNF motifs I–III and IV–VI form two semi-autonomous modules, both of which are bound to DNA in the reported structure (24).

Our most recent work has focused on the determination of preferred nucleic acid and/or protein substrates of RapA. Excess RapA was previously shown to produce complex effects on *in vitro* transcription, which included inhibitory effects at 'early' timepoints and a significant increase in the number of completed transcriptional rounds in prolonged *in vitro* transcription reactions, which was attributed to RapAs remodeling of DNA–RNA polymerase–RNA ternary complexes (23). In this study—given that the interaction of RapA with the polymerase is well established—using primarily purified native RapA (21) at a 'physiological' (1:1) molar ratio with the polymerase, we have conducted experiments in order to clarify the general mechanistic aspects of this remodeling. Our work presents multiple, independent lines of evidence indicating that RNA is a key substrate of RapA. Our biochemical data, supported by a homology model of the RapA NTPase domain–DNA complex, suggest that this RNA-remodeling activity of RapA may be in addition to its DNA-binding activity. Our results are consistent with a model in which RapA promotes RNA release from DNA–RNA polymerase–RNA ternary complexes. Taken together, our data indicate a novel RNA remodeling activity for RapA, a representative of the SWI/SNF protein superfamily. This finding could potentially deepen our understanding of the functions of all SWI/SNF proteins, and may point to yet-unidentified activities of eukaryotic SWI/SNF proteins.

MATERIALS AND METHODS

Enzymes

Native RapA was isolated as described (19,21). Core RNA polymerase, RNA polymerase holoenzyme, NusA, S1 and Hfq were purified as described (25). Recombinant RapA was obtained by amplification of the *rapA* gene from MG1655 chromosomal DNA using MS152 (5′-CGT TAACGGATCCGACCCGGGCCTTTTACACTTGGT CAACGCTGGATCAG) and MS153 (5′-ATTGTCCCG GGCTGCAGCCGACCGCTCGGCTTGTTGACCACC ATAATATG) DNA primers, subcloning the resulting PCR product into the XmaI site of the vector pQE32 (Qiagen), and overexpression and purification of the recombinant His-tagged protein as described (22). Over 90% of the *rapA* sequence (including 100% of the SWI/SNF homology regions) was confirmed by DNA sequencing and found to be identical to that in the NCBI database.

'In vitro transcription experiments' were carried out, generally, as described (23), with the exceptions that, when indicated, denaturation of the samples by boiling following the addition of a 1/5 reaction volume of $5 \times$ Stop solution (50% glycerol, 100 mM EDTA, pH 7.5, 0.1% bromphenol blue) was omitted, and the final RNA polymerase holoenzyme concentrations were 0.05–0.06 mg/ml. The RNA polymerase–(native)RapA ratio in all described experiments (unless indicated otherwise in the figure legend) was 1:1. No detectable differences (in *in vitro* transcription or other enzymatic assays described in this study) were found between the 1:1 RNA polymerase RapA complexes obtained during the course of previously described purification procedures (19,21,25) and the same complexes reconstituted from purified RNA polymerase and RapA. All described experiments utilized native RapA, with the exception of the experiments described in Figure 5B, which were carried out with recombinant (His-tagged) RapA. Recombinant (His-tagged)RapA^{K183A} (23) was isolated as described for wild-type recombinant protein (22). Reaction buffers and the supercoiled plasmid DNA templates are specified in the figure legends. Kinetics of RNA synthesis were monitored, generally, as previously described (23) for the reactions initiated by the addition of rNTPs [see Ref. (23); Figure 5B therein], except that the final concentration of each rNTP was 0.2 mM and the RNA polymerase holoenzyme concentration was 0.05 mg/ml.

Electrophoretic mobility shift assay (EMSA)

Protein–RNA binding assays. Proteins and the ^{32}P-labeled purified RNA probe (typically present at 500–1000 c.p.m./20 μl binding reaction) were mixed in 50 mM Tris–HCl, pH 7.5, containing 5 mM MgCl$_2$, 0.5 mg/ml BSA and 200 mM NaCl. The binding reactions were incubated for 5 min at room temperature, and 5 μl of loading buffer (50% glycerol supplemented with 0.05% bromphenol

blue) was added to each binding reaction. Aliquots of 2–8 μl were then analyzed on 8% polyacrylamide gels containing 0.5× TBE or 2× TBE, as described in the legend to Figure 2. BioMax ML film was exposed to dried gels (typically 6–18 h at −70°C) with BioMax MS screens.

DNA–RNA EMSA-binding experiments. Synthetic RNA oligonucleotides were obtained from Dharmacon. Nucleic acid probes were labeled at the 5′-end using T4 polynucleotide kinase (USB) and [Gamma ^{32}P] ATP (MP Biomedicals), according to the USB protocol. Following the end-labeling procedure, the RNA probes were gel-purified on a denaturing 20% polyacrylamide gel (National Diagnostics). The gel-purification procedure for RNA probes was as follows. After PAGE, X-ray film was exposed to a 'wet' gel that had been covered with plastic wrap. Full-length RNA bands were visualized, marked and cut from the gel. The polyacrylamide gel slice containing the end-labeled RNA was then manually homogenized in an RNase-free, 1.5 ml Eppendorf tube-size disposable homogenizer, typically using 200 μl of 2 × TBE. Following the 2–3-min homogenization, the slurry was immediately applied on a microcentrifuge filter vial (Ultrafree-DA; Millipore), and the flow-through was aliquoted and stored at −70°C. Synthetic DNA oligonucleotides were either gel- or cartridge-purified. DNA oligonucleotides obtained from two independent vendors (Invitrogen and Sigma Genosys) were tested in the DNA–RNA binding experiments, with similar results. Key experiments (including the experiments described in Figure 7B, C and Figure S5) were carried out with synthetic DNA oligonucleotides obtained from Invitrogen. DNA and RNA oligonucleotides were incubated for 5 min at room temperature in the buffers specified in the Figure 7A legend, mixed with 1/5 volume of a loading buffer containing 50% glycerol (Sigma Ultrapure) and 0.01% bromphenol blue and analyzed by PAGE using 20 × 20 cm, 1-mm thick 12% polyacrylamide gels, which were cast and run using the buffers specified in the legend to Figure 7A. Typically, PAGE was performed at 20 milliamps/gel. Tris–Borate–EDTA (TBE) buffer from two independent vendors (KD Medical and MP Biomedicals)—obtained either as a 10× concentrate (KD Medical, MP Biomedicals) or a premixed powder (MP Biomedicals)—was tested, with similar results. The pH in different batches of commercially available 10× TBE was 7.8–8.3.

'Immobilized DNA–RNA templates' were constructed by incubating agarose-bound polynucleotides (Amersham-Pharmacia) with soluble DNA (either $[dA]_{20}[dC]_4[T]_{20}$ or $[dA]_{20}[dG]_4[T]_{20}$; Invitrogen) or RNA (5′-CCUGUUUUUAAGGAGUGUCGCCAGAGGCC GCGAUG$[A]_{18}$-3′; Dharmacon) ^{32}P-labeled synthetic oligonucleotides (0.05–0.1 A_{260} U/ml) at room temperature, followed by extensive washing with 50 mM Tris–HCl (pH 7.5), 200 mM NaCl, 5 mM $MgCl_2$. One hundred microliters of binding reactions containing ~20 μl of agarose-bound DNA–RNA complexes were incubated with gentle agitation at room temperature for 30 min, unless otherwise indicated in the figure legends, and the
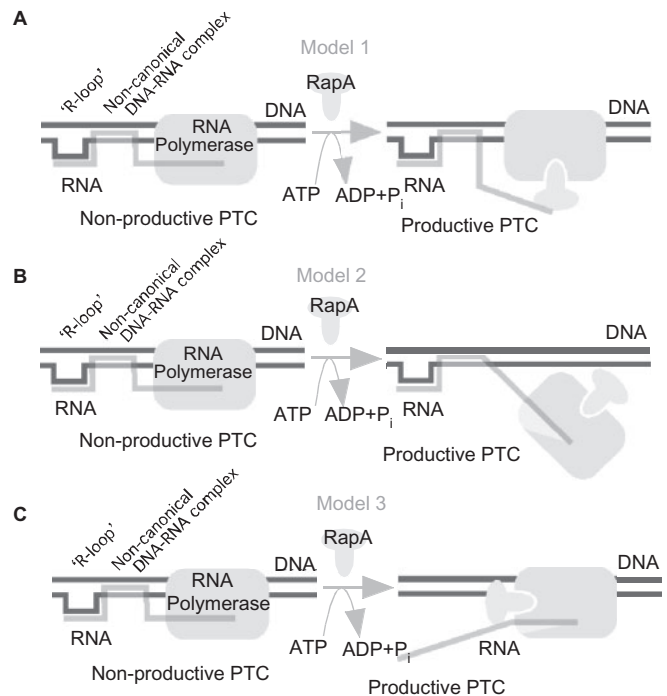

Figure 1. Three plausible mechanisms explaining the RapA-mediated remodeling of non-productive post-termination complexes (23). See text for a detailed description of each of the indicated models.

nucleic acid content of the aqueous phase was determined. The reaction ingredients were as described in the legend to Figure 7B and Figure S4.

RESULTS

Previously, it was demonstrated that excess RapA can promote transcriptional cycling via some undetermined means of remodeling post-termination, DNA–RNA polymerase–RNA ternary complexes (23). However, it is unclear which component(s) of the ternary, post-termination DNA–RNA polymerase–RNA complex (PTC) are targeted by RapA. In principle, RapA may (i) facilitate the release of nascent RNA from RNA polymerase (Model 1, Figure 1A), (ii) promote the release of RNA polymerase (with or without nascent RNA) from DNA (Model 2, Figure 1B), and/or (iii) stimulate transcriptional cycling by means of disrupting non-productive DNA–RNA complexes, irrespective of either the DNA-bound or free status of the polymerase (Model 3, Figure 1C). [Factors that may potentially hinder transcriptional cycling are summarized in our recent study (26).] (iv) Alternatively, RapA activity can be described as a combination of Models 1 through 3 (particularly 1 and 3). In this study, we carried out experiments to clarify the mechanistic aspects of RapA catalysis in terms of its general compatibility with one or more of the aforementioned models.

Model 1

Purified system. First, we tested the effect of RapA on the stability of RNA polymerase–RNA complexes in
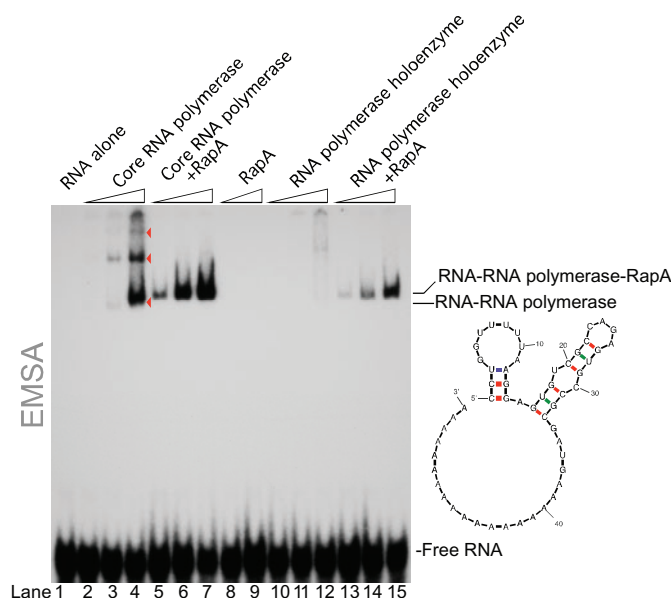
Figure 2. RapA promotes interaction of RNA polymerase with RNA. EMSA gel illustrating the effect of RapA on interaction of the core RNA polymerase (lanes 2–7) or the RNA polymerase holoenzyme (lanes 10–15) with end-labeled 55-nt RNA incorporating stem-loop structures and an rA18 tail. EMSA-binding experiments were carried out as described in Materials and Methods section. Other RNA probes of varied length and structure (see text for details) produced similar binding patterns, indicating a greatly increased RNA-binding affinity of the polymerase in the presence of RapA. Quantitation of the RNA polymerase (holoenzyme)-bound RNA in the presence or absence of RapA (lanes 15 and 12) indicated a >20-fold increase in RNA-binding affinity in the presence of RapA. Note that RapA abolishes the formation of multimeric RNA polymerase–RNA complexes formed by the core RNA polymerase (indicated with arrowheads).

a purified system (in the absence of rNTPs and DNA) using PAGE-based electrophoretic mobility shift assays (EMSA) (Figure 2). The core RNA polymerase showed higher RNA-binding affinity than that of the RNA polymerase holoenzyme (Figure 2; compare lanes 1–4 and lanes 10–12), and RapA showed no detectable RNA-binding activity under these experimental conditions (Figure 2; lanes 8 and 9). Formation of the RNA polymerase–RapA complex was accompanied by a significant increase in the RNA-binding activity of the complex compared to that of RNA polymerase alone; the effect was particularly dramatic for the RNA polymerase holoenzyme (Figure 2; compare lanes 10–12 and lanes 13–15). We tested several different RNAs of varied length and structure and obtained similar results using a short, 55-nt RNA consisting of two stem-loop structures followed by an 18-nt (rA) tail (Figure 2) [RapA ATPase activity was not affected significantly by the presence of an excess of this secondary structure-containing RNA (Supplementary Data; Figure S1), in agreement with the previously reported results indicating a lack of effect of Poly[rA] on RapA-mediated ATP hydrolysis (19)], rA_{20} (Supplementary Data; Figure S3) and the bacteriophage lambda RNA I (data not shown). We also compared side-by-side the affinities of the RNA polymerase holoenzyme–RapA complex to RNA and

DNA probes with matching (save U/T transitions) nucleotide sequences (Supplementary Data; Figure S2). These experiments further confirmed that the complex is capable of binding both DNA and RNA, with mild (approximately 2-fold) preference of an mRNA-like RNA probe over a similar DNA probe (Supplementary Data; Figure S2).

In vitro transcription system. It is conceivable that if RapA were to promote the release of RNA from transcription complexes, RapA–RNA intermediates might be detected during fractionation of the components of *in vitro* transcription reactions by PAGE. The experiments described below were carried out to detect such hypothetical RapA–RNA and/or RNA polymerase–RapA–RNA intermediates. Typically, *in vitro* transcription reactions are denatured by boiling before their RNA content can be analyzed by PAGE. Bypassing the boiling step, we fractionated the content of entire *in vitro* transcription reactions by PAGE on 6% polyacrylamide–urea gels (Figure 3). This approach revealed unique protein–RNA complexes present only in the reactions containing RapA (Figure 3, complexes 'B'; the sensitivity to boiling distinguishes these complexes from RNA transcripts). We tested whether these RapA-specific complexes were promoter- or terminator-specific and found that they were detected irrespective of the type of DNA template used in the reactions (Figure 3A–D).

To determine the composition of these complexes, we used two independent experimental approaches. In the first approach (an immunoassay), proteins and protein–nucleic acid complexes were electroeluted from the gel onto a membrane which was subsequently incubated with either RNA polymerase-specific or RapA-specific polyclonal antibodies (in parallel reactions). In the second approach, RapA-specific complexes ('B' complexes in Figures 3 and 4), identified after exposure of X-ray films to 'wet' polyacrylamide gels, were excised from the gel; the gel slices were homogenized in Laemmli sample buffer and their content was analyzed on silver-stained SDS–polyacrylamide gels. Both approaches produced consistent results, indicating that the complexes in question contain a sole polypeptide—RapA—and RNA (the results of an immunoassay are shown in Figure 4). We also analyzed the nature of the RapA-associated RNA transcripts and determined that they are represented predominantly by a major promoter-specific RNA transcript, unique for each of the two sets of templates used (data not shown).

Analysis of the kinetics of the RapA–RNA adduct formation indicated nearly instantaneous RapA–RNA interaction; there was a good correlation between the yield of RapA–RNA adduct and that of promoter-specific transcript in reactions with or without RapA (Figure 5A). Excess BSA failed to significantly reduce levels of RapA–RNA adduct (Supplementary Data; Figure S4B) suggesting that the transcript interacts specifically with RapA, and stable RapA–transcript complexes were formed in *in vitro* transcription reactions carried out in various buffers, including 2× TBE containing 5 mM magnesium chloride (Supplementary Data; Figure S4A). [This buffer
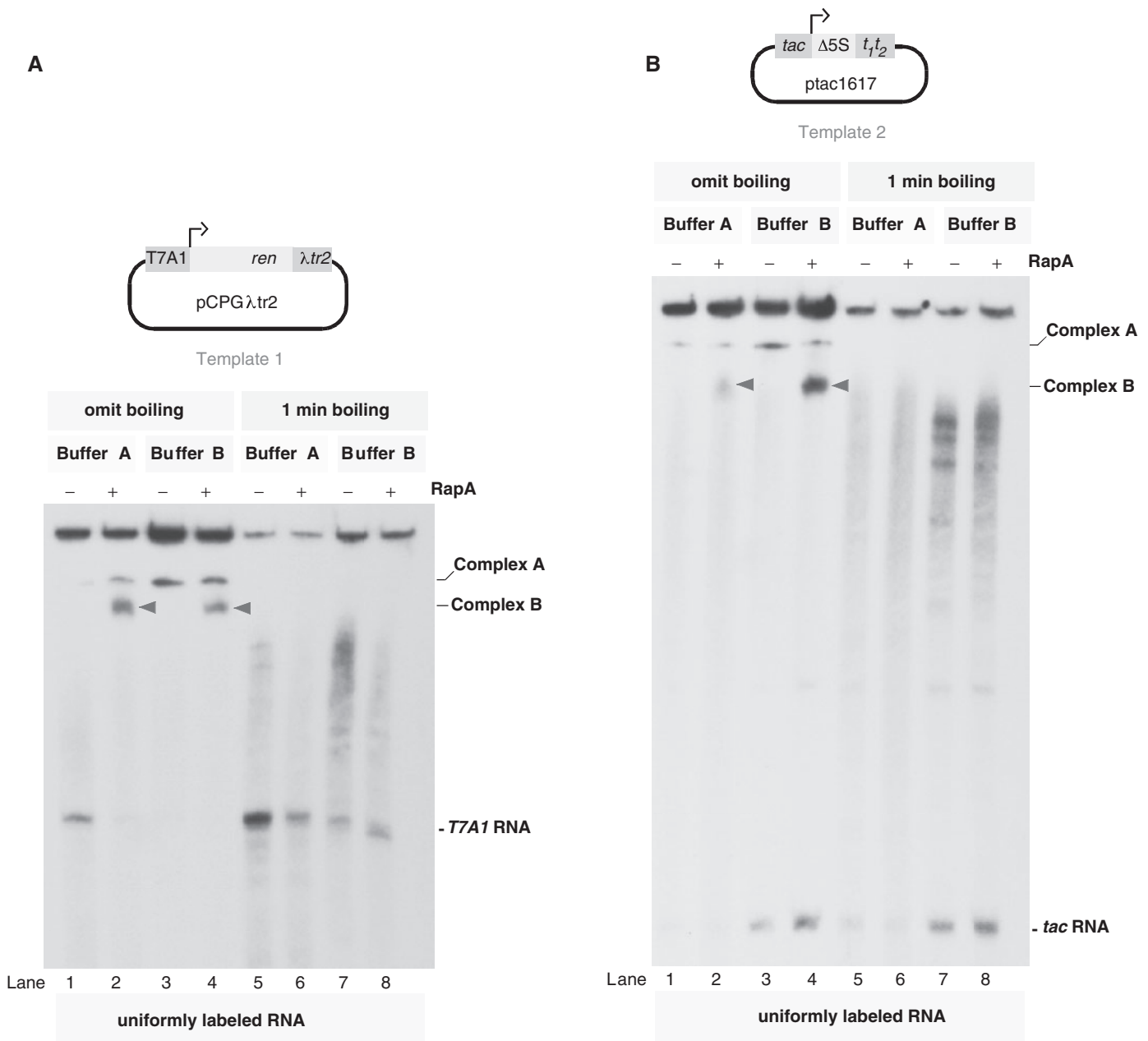
Figure 3. Formation of stable *in vitro* transcription reaction intermediates in the presence of RapA. *In vitro* transcription reactions with supercoiled DNA templates were carried out, in general, as previously described (23), except that 1 mol purified native RapA per mole of the RNA polymerase holoenzyme (0.05–0.06 mg/ml) was used throughout this study, unless indicated otherwise in the figure legends. Reaction products of 15 min *in vitro* transcription reactions (with or without 1-min boiling following the addition of a Stop solution) were fractionated on 6% PAA–urea gels. Buffer A: 50 mM MOPS (pH 7.0), 5 mM MgCl$_2$; Buffer B: 50 mM Tris–HCl (pH 7.9), 10 mM MgCl$_2$, 200 mM NaCl, 1 mM dithiothreitol. (A–D) Formation of stable RapA-specific transcription reaction intermediates does not depend on the nature of a supercoiled DNA template. Templates 1 and 3, which carry the *T7A1* promoter and either lambda *tr2* or *t3te* terminators are described in Ref. (27). Template 2, which carries the *tac* promoter and *t1t2* terminator is described in Ref. (23). Template 4, which carries the lambda *Pr* promoter, but is otherwise similar to Template 2, was constructed by substituting the *tac* promoter in Template 2 samples were initiated by the addition of rNTP mix containing either [Alpha-^{32}P] ATP (lanes 9–16) or [Gamma-^{32}P] ATP plus T4 PNK (0.2 U/μl) (lanes 1–8). The stock solutions of both radiolabeled nucleotides (see Materials and Methods section) were diluted (typically, 120-fold and 9-fold, respectively) to obtain comparable incorporations of the label in the two sets of samples; the final rNTP concentrations remained the same ([ATP] = [UTP] = [GTP] = [CTP] = 0.2 mM). The formation of stable RapA-specific reaction intermediates with all four different DNA templates suggests that the effect is not template-specific.
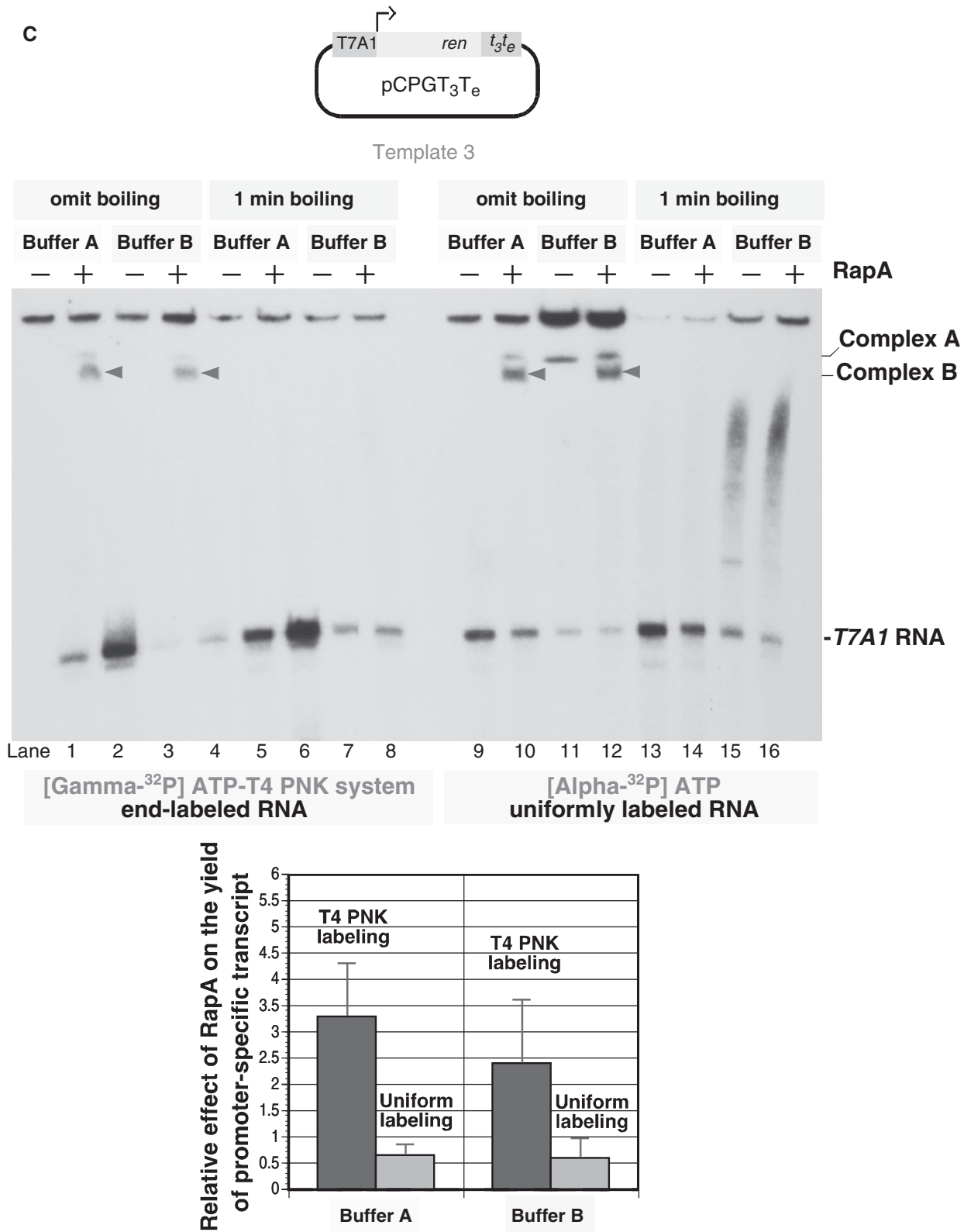
c

Template 3

[Gamma-^{32}P] ATP-T4 PNK system
end-labeled RNA

[Alpha-^{32}P] ATP
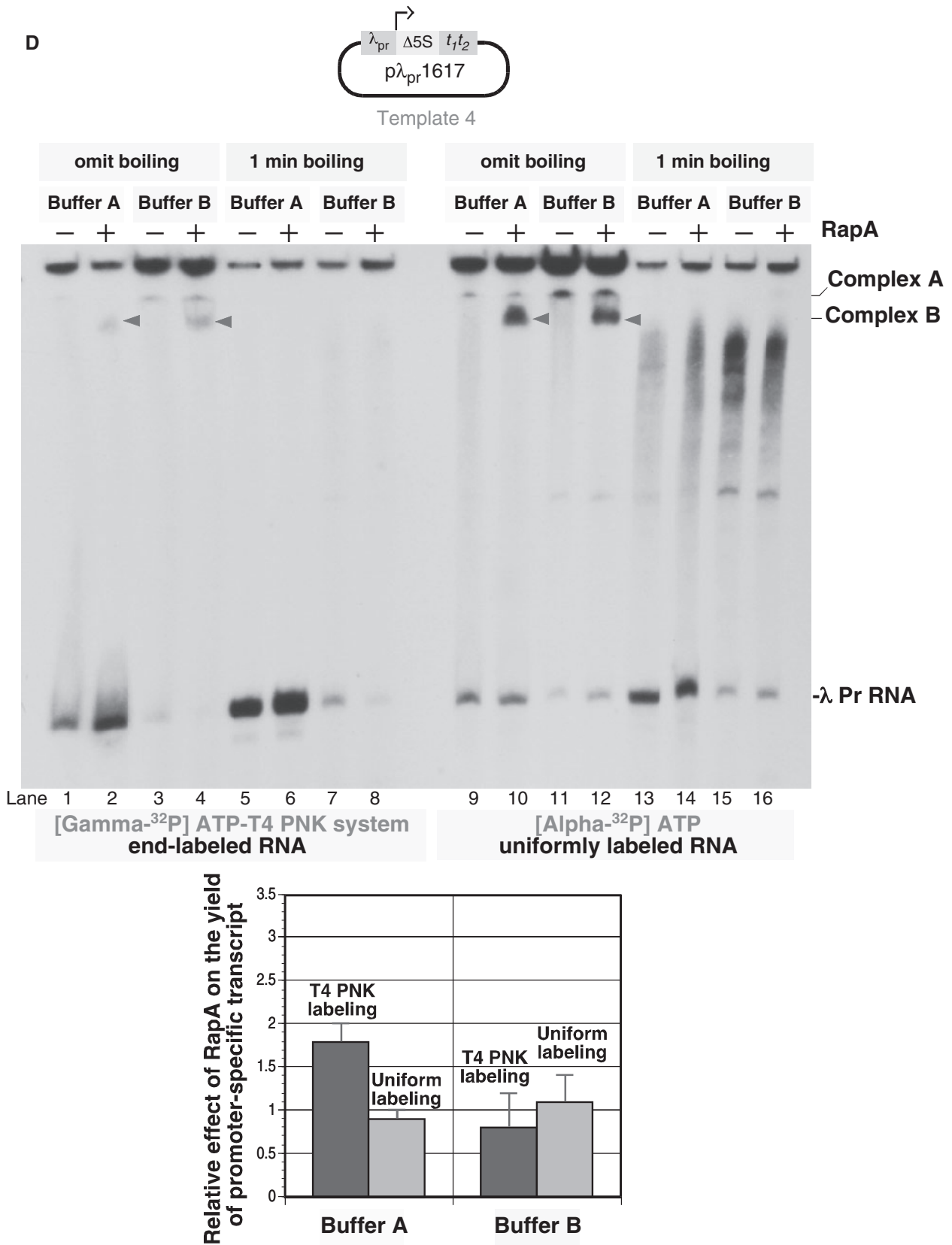uniformly labeled RNA

Figure 3. Continued.
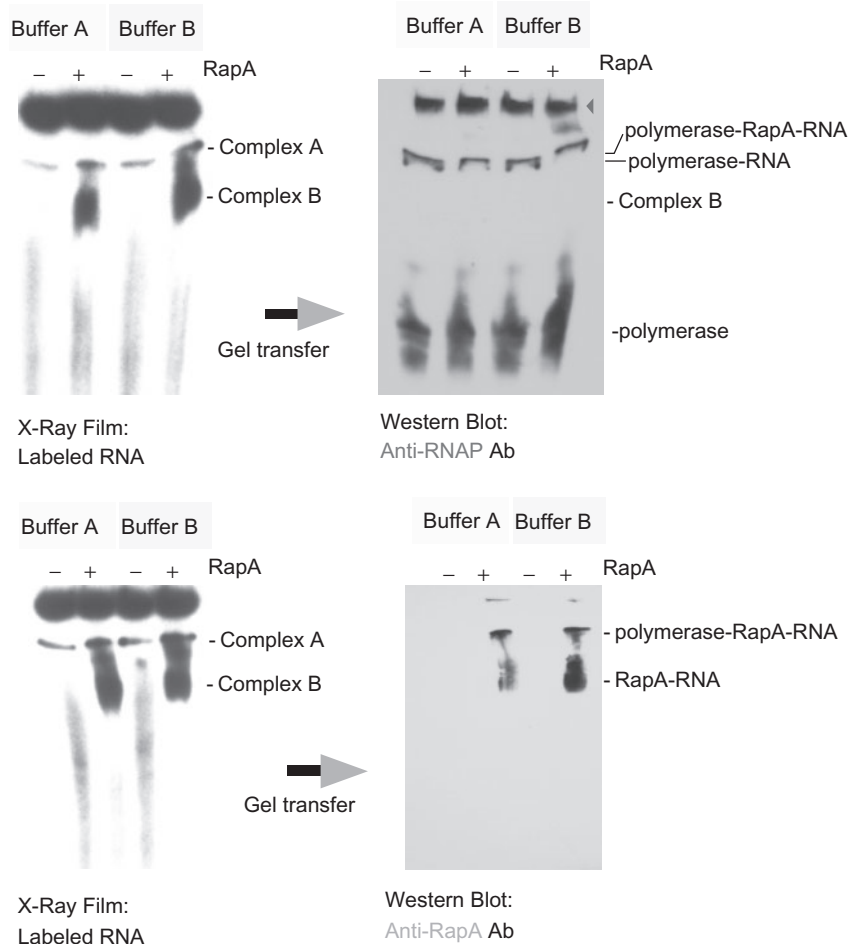
Figure 3. Continued.

Figure 4. Immunological characterization of the composition of the RapA-specific *in vitro* transcription reaction intermediates. *In vitro* transcription reactions similar to those described in Figure 3 (Template 2) were carried out, and the entire reactions were fractionated on 6% polyacrylamide–6 M urea gels (National Diagnostics). Following the electrophoresis, X-ray films were exposed to 'wet' gels to visualize ^{32}P-labeled RNA transcripts (left panels). Next, the gel contents were electroeluted onto Hybond P membranes (Amersham Pharmacia Biotech), and the membranes were immunostained with either RapA- or RNA polymerase-specific antibodies in independent, parallel reactions (right panels). Western blotting was performed as described (22). DNA-associated RNA polymerase (indicated with an arrowhead), free RNA polymerase, RNA polymerase–RNA and RapA–RNA complexes are indicated.

was tested in addition to 'standard' reaction buffers (see Materials and Methods section) to validate the comparison of data obtained from *in vitro* transcription studies with those from PAGE-based binding assays (see below)].

We next tested whether the disruption of RapA ATPase activity by the Lys183Ala mutation (23) could have an effect on the formation of the RapA–RNA adduct. These experiments have demonstrated, in general, reduced ability of the RapA[Lys183Ala] mutant to engage RNA (Figure 5B; compare lanes 2 and 3, 8 and 9, 11 and 12); yet mutant RapA was capable of forming protein–RNA complexes (indicated with red arrowheads in Figure 5B) under certain, presumably 'optimal' conditions (at 37°C and with relatively long transcripts produced from Template 1; Figure 5B, lanes 5 and 6). It is tempting to speculate that the increased level of RNA polymerase–RapA[Lys183Ala]–transcript complex compared to that in the reaction with wild-type RapA, which correlated inversely

with the levels of 'free' promoter-specific transcripts in the indicated reactions, may be due to inability of the mutant RapA to efficiently remove the transcript from the polymerase (Figure 5B, bottom panel).

To obtain further evidence for RapA-mediated RNA remodeling during transcription, we used T4 polynucleotide kinase (T4 PNK) as a gauge for the availability of the 5′-terminus of nascent RNA in *in vitro* transcription reactions with or without RapA. We transiently end-labeled the 5′-termini of promoter-specific transcripts in medium-duration (15 min) *in vitro* transcription reactions and compared the ratios of the yields of promoter-specific transcript in reactions with or without RapA with those in otherwise identical reactions (sans T4 PNK) utilizing conventional, uniform RNA labeling (Figure 3C and D, graphs). The result of this set of experiments indicated that there was a general (buffer- and template-independent) increase in the efficiency of the 5′ end-labeling of nascent RNA in the presence of RapA
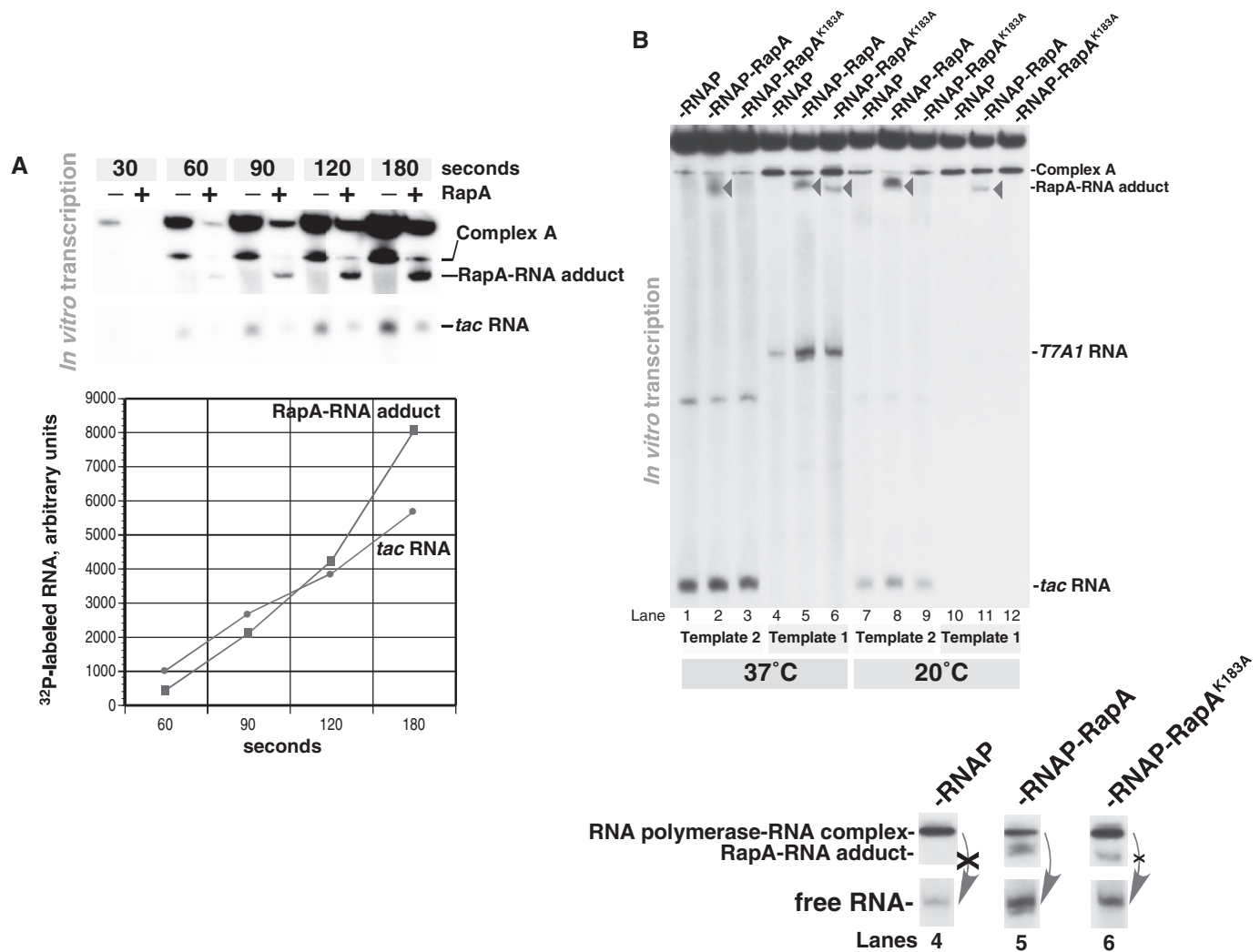
Figure 5. Kinetics of the RapA–RNA adduct formation and the effect of the RapA Lys183Ala mutation on the RapA–RNA interaction. *In vitro* transcription experiments were as described in the Materials and Methods section; denaturation of the samples by boiling following the addition of a stop solution was omitted. (**A**) Kinetics of the RapA–RNA adduct formation. *In vitro* transcription reactions were initiated by the addition of rNTPs (the final concentration of each rNTP was 0.2 mM) following a 15-min preincubation of the enzyme(s) with supercoiled DNA at 37°C. (**B**) Effect of the RapA Lys183Ala mutation [resulting in disruption of the RapA ATPase activity (23)], on the RapA–RNA adduct formation. Bottom panel: highlight of the results of the experiment.

(Figure 3C and D, graphs; the sole exception being Template 4 with Buffer 'B') indicating RNA remodeling consistent with either a full transcript release or possibly partial peeling of the transcript's 5′-terminal segment from the transcription complex.

Model 2

This model was considered in our earlier study (23), and it was based on the speculation that RNA polymerase 'trapped' on DNA cannot disengage from it in order to reinitiate new cycles of transcription efficiently. If RapA were indeed to promote transcriptional cycling by displacing RNA polymerase from DNA, under most circumstances [the exception being a nearly instantaneous transfer of the polymerase from the terminator to the promoter section in the DNA template, which, at least in theory, cannot be entirely ruled out due to possible

co-alignment of these two sections in supercoiled DNA (see Ref. 23; Figure 8 therein)] this should be accompanied by a measurable increase in the fraction of free RNA polymerase in the system. We tested this possibility using PAGE- and ultracentrifugation-based techniques. In the first, PAGE-based assay, *in vitro* transcription reactions carried out to stationary phase (with or without RapA present) were fractionated on non-denaturing 5% polyacrylamide gels in the presence of magnesium, and the amounts and subunit composition of the DNA-bound polymerase were determined (Figure 6). These experiments showed no detectable reduction in the amount of DNA-associated RNA polymerase in the presence of RapA (Figure 6, densitogram; compare the levels of the large RNA polymerase subunits in reactions with or without RapA). Also, this set of experiments showed that >85% of RapA dissociated from the DNA-bound RNA
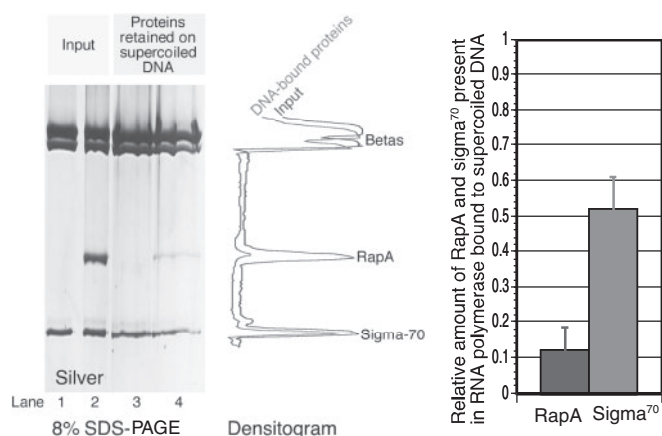
Figure 6. Lack of the RapA effect on the amount of DNA-bound RNA polymerase in *in vitro* transcription reactions with supercoiled DNA. *In vitro* transcription reactions carried out for 15 min at 37°C in the presence or absence of RapA were fractionated on non-denaturing 5% polyacrylamide gels, which were cast and run using 2× TBE, and the amounts of individual RNA polymerase subunits retained on supercoiled DNA were determined from quantitated SDS gels, as described in the text. Quantitated levels of RapA and sigma[70] retained by the DNA-bound polymerase are shown in the right panel. Results of this experiment indicate that RapA does not reduce the fraction of DNA-bound RNA polymerase during *in vitro* transcription, contrary to the previously proposed model (23).

polymerase, while >50% of the sigma[70] subunit was retained by the DNA-bound enzyme (Figure 6, graph). In the second approach, *in vitro* transcription reactions were subjected to ultracentrifugation in order to determine the fractions of DNA-bound and free RNA polymerase in reactions with or without RapA. Similarly, these experiments showed no effect of excess RapA on the ratio of free and DNA-bound RNA polymerase in the system (data not shown). Furthermore, a number of other independent experiments, which assessed the amount of DNA-associated RNA polymerase in reactions with or without RapA consistently showed no effect of RapA on the amount of DNA-associated polymerase (for example, see Figure 4 above).

Model 3

Nascent RNA may form DNA–RNA complexes potentially inhibitory to transcription, such as DNA–RNA duplexes and, possibly, non-canonical DNA–RNA complexes, such as DNA–RNA triplexes (28–30). Our recent study implied that potential non-productive interactions by nascent RNA may represent a primary obstacle to continuous transcriptional cycling (26).

Test of the effect of RapA on the stability of DNA–RNA double-strand complexes. Previously we reported that RapA showed no detectable DNA helicase activity with duplex DNA templates (19). During the course of the next set of experiments, we tested RapAs hypothetical DNA–RNA helicase activity using a system with immobilized DNA–RNA duplexes. Because the effects of RNA polymerase and its accessory proteins on the stability of DNA–RNA double-strand complexes, to the best of

our knowledge, have not been tested before, we used our previously described technique for purification of the polymerase and its accessory proteins in a single purification procedure (25) to isolate multiple proteins in order to test their effect on the stability of such complexes. With immobilized duplex RNA–DNA templates, in which a 55-nt RNA probe consisting of a stem-loop structure followed by an rA_{18} tail is hybridized to Oligo(dT)-agarose, RNA polymerase showed some limited ability to displace RNA into the soluble phase in the presence of ATP (Supplementary Data, Figure S5, lane 2), possibly due to rA_n synthesis with Oligo(dT) DNA as a template. The transcriptional activity of *E. coli* RNA polymerase with single-stranded DNA templates has been reported (31). However, none of the tested proteins, including RapA, even marginally enhanced or otherwise altered this activity (Supplementary Data, Figure S5).

Test of the effect of RapA on the stability of DNA–RNA putative triple-strand complexes. The existence of this type of interaction has not been definitively proven *in vivo*. However, its *in vitro* study may arguably yield potentially new and interesting results. A pioneering work by Roberts and Crothers presented evidence for the formation of duplex DNA-single-stranded RNA triplexes *in vitro* (28). Because of the overall scarcity of data regarding specific conditions for DNA–RNA triplex formation, we first set out to confirm the formation of non-canonical DNA–RNA complexes in a PAGE-based binding assay that allows unambiguous detection of complexes between unmodified and/or untethered templates. We have chosen to test the optimal conditions for rA–dA–dT interaction; the rationale being: (i) the likely similarity of rA–dA–dT triplexes to dA–dA–dT DNA triplexes, which are textbook examples of Hoogsteen complexes proven beyond reasonable doubt, (ii) the study of putative rA–dA–dT triplexes would be complementary to already existing data (28) and (iii) homo-dA/dT tracts are relatively common in both prokaryotes and eukaryotes, particularly under the promoter and terminator regions.

Under 'standard' EMSA conditions (in 0.5× TBE) model DNA templates (which followed the basic design introduced in the study referred to above) incorporating $(dA/dT)_{20}$ homoduplexes (with varied composition of the 4-nt loop in DNA) showed no interaction with rA_{20}, as expected (Figure 7A, Gel 1). However, an increase in the ionic strength (to 2× TBE) led to the formation of stable DNA–RNA complexes; the $(dA/dT)_{20}$ homoduplex was essential to the interaction (Figure 7A, Gel 2), and the increase in the length of the dA/dT tract to $(dA/dT)_{40}$ resulted in an expected gel-retardation effect (Figure 7A, Gel 2; compare lanes 2 and 3 with lanes 14 and 15). Interestingly, the composition of the 4-nt loop in DNA contributed to the strength of the interaction, with C_4 or GATC being more preferred than G_4. Stable DNA–RNA complexes (putative DNA–RNA triplexes) were formed when 2× TBE was supplemented with 5 mM magnesium chloride (Figure 7A, Gel 3); the reduced mobility of the nucleic acid probes may be due to Mg^{2+}–nucleic acid interaction; however the formation of rA–rA–dT triplexes under these conditions cannot be entirely ruled out.
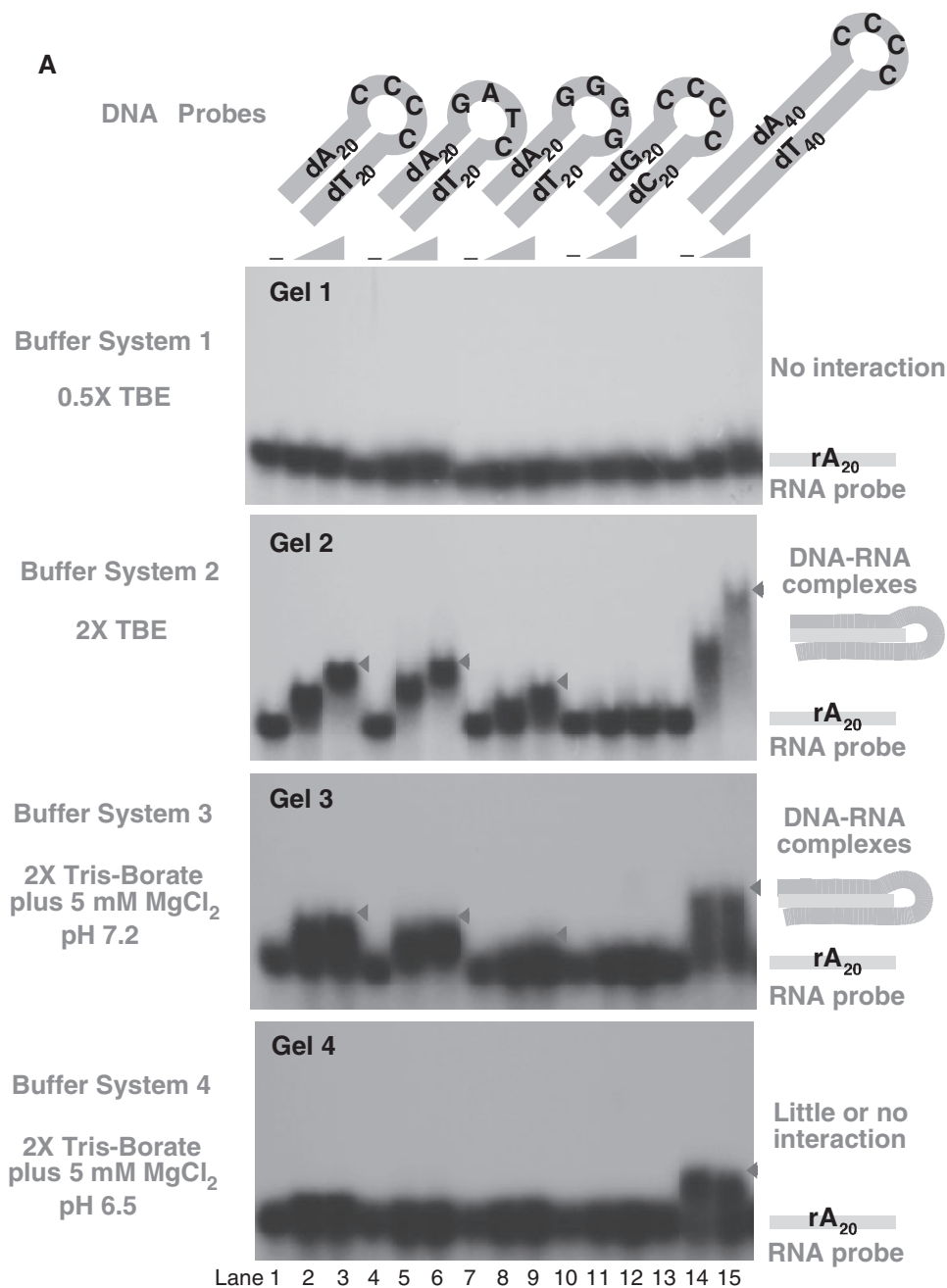
Figure 7. RapA promotes ATP-dependent separation of RNA from DNA in putative non-canonical DNA–RNA complexes. (**A**) PAGE-based demonstration of a non-canonical interaction between the double-stranded DNA probes (shown at the top) and $(rA)_{20}$ RNA. The buffers used for the sample preparation, gel casting and running are indicated at the left. The 10 µl binding reactions in lanes 2 and 3, 5 and 6, 8 and 9, 11 and 12, 14 and 15 contained, respectively, 40 and 160 pmol DNA. Nucleic acid probes were purified as described in the Materials and Methods section. The overall design of nucleic acid probes used in this set of experiments mimics that described in Ref. (28). Note that the DNA probe shown in lanes 1–3 ($5'$-$dA_{20}dC_{4}dT_{20}$) was utilized in the experiments with immobilized non-canonical DNA–RNA complexes described below. (**B**) RapA promotes destabilization of putative DNA–RNA triplexes in an ATP-dependent manner. A schematic of the experiment is illustrated in the top panel. RNA polymerase, S1, Hfq, NusA and RapA were isolated as described in the Materials and Methods section. Reaction components were present in the following concentrations: RNA polymerase and transcription factors, 200 nM; Tris–HCl (pH 7.5), 50 mM; NaCl, 200 mM; $MgCl_{2}$, 5 mM; ATP, 0.2 mM. Kinetics of ATP-dependent (red bars) or ATP-independent (blue bars) disruption of DNA–RNA templates by RNA polymerase (lane 2), RapA (lane 5) or a 1:1 RNA polymerase–RapA complex (lane 6) in 10-min (open bars), 30-min (hatched bars) and 90-min (solid bars) reactions. Controls included: no proteins (lane 1); the polymerase-associated RNA-binding factor NusA (lane 3); NusA plus RNA polymerase (lane 4); the ribosomal protein S1 (lane 7); the Sm-like ATPase Hfq (lane 8) and S1 plus Hfq (lane 9). (**C**) Separation of RNA from DNA in putative triplexes by the RNA polymerase–RapA complex under conditions of excess RapA. Core RNA polymerase, 100 nM; RapA, 800 nM; Tris–HCl (pH 7.5), 50 mM; NaCl, 200 mM; $MgCl_{2}$, 5 mM; ATP, 2 mM. Approximately 4000 c.p.m. of ^{32}P-labeled DNA was used per reaction; data represent the results of four independent sets of experiments. Coomassie-stained samples of core RNA polymerase (5.6 µg) and RapA (1.4 µg) used in this experiment are shown below.
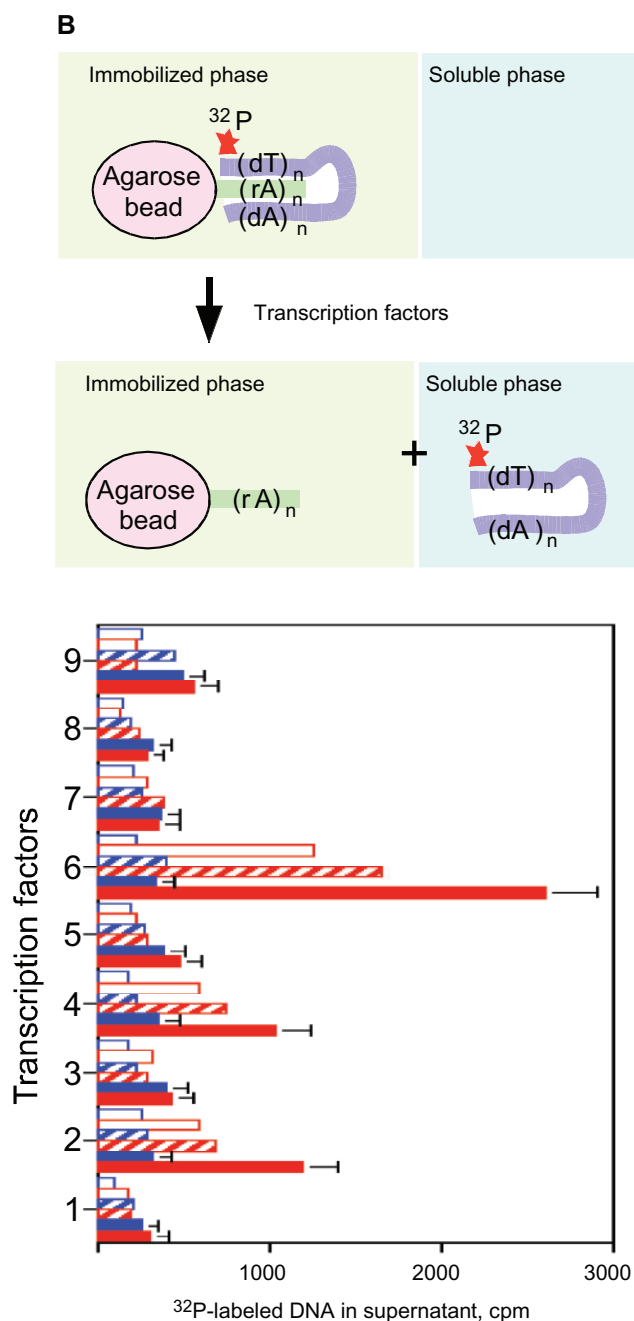
B

C

^{32}P-labeled DNA in supernatant, cpm

Figure 7. Continued.

The reduced interaction at lowered pH (Figure 7A, Gel 4) suggests that $O^-\ldots H$ hydrogen bonds may be essential for DNA–RNA interaction. Next, we tested RNA probes in which the RNAs rA_{18} tract is followed by a stem-loop structure (thus, the RNAs 3′-end is blocked by a 'non-interactor' extension); these templates also formed stable complexes with the indicated DNA probes under 'optimal' conditions—at relatively high salt concentrations, in the presence of magnesium. A detailed description of these experiments is provided as Supplementary Data (Figure S6). In general, our PAGE-based study produced
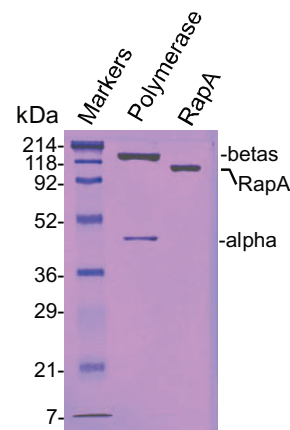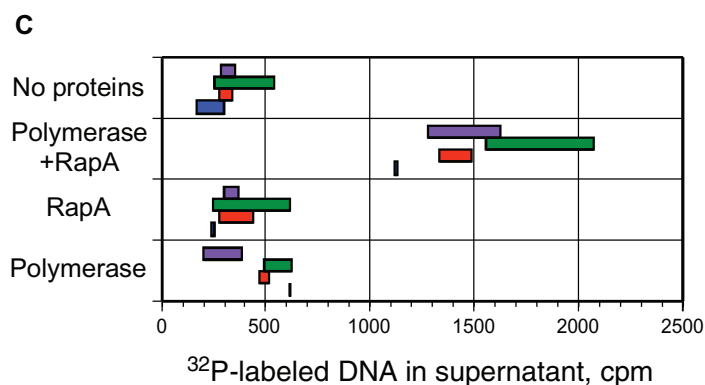
results consistent with those reported by others (28,29), with relatively high salt concentrations and magnesium promoting non-canonical interactions, as reported (29).

Next, we constructed immobilized DNA–RNA complexes, in which $5'dA_{20}dC_4dT_{20}$ DNA was immobilized on Poly (rA)–agarose, to test the effect of RapA on their stability. At 200 mM NaCl [in 50 mM Tris–HCl, pH 7.5, 5 mM $MgCl_2$ (Buffer C)]—the 'optimal' conditions for the earlier described transcription-stimulatory activity of RapA (23,26)—the DNA probe ($5'dA_{20}dC_4dT_{20}$) formed a stable complex with Poly(rA)–agarose, as expected.

Figure 8. Predicted partial structure of the RapA NTPase/(putative) DNA-binding module. RapAs amino acid sequence was threaded into the SsoRad54–DNA structure via the SWISS-MODEL Protein Modeling Server (32–34). (**A**) Homology between SWI/SNF subdomain 'I' of RapA and that of the *Sulfolobus solfataricus* Rad54 homolog (SsoRad54). Identical and homologous amino acids are marked by, respectively, red and blue boxes. A limited sequence homology between SWI/SNF subdomain 'I' of RapA and an RNA-binding, or 'S1'-module of the ribosomal protein S1 is also indicated (dashes, colons). The RapA SWI/SNF subdomains are shown schematically at the top; the aligned segments represent the section that yielded the homology model shown below. (**B** and **C**) Predicted structure of the RapA NTPase/(putative) DNA-binding module (sticks and mesh shown in color) superimposed with the homologous domain of SsoRad54 (gray mesh) bound to DNA (shown as CPK spheres), as reported by the Hopfner group (24). (**D**–**G**) Predicted partial structure of the RapA NTPase module (shown in color) superimposed with the complete SsoRad54 ATPase core–DNA complex (shown in gray scale) (24). Key amino acid changes in the RapA NTPase module relative to that of SsoRad54 are highlighted as CPK spheres. Lys183 (a highly conserved residue present in both proteins), alanine substitution of which results in significantly reduced ATPase activity in purified RapA (23), is shown in salmon pink. Several amino acids present in RapA but not found in SsoRad54, such as Arg222, Arg221, Tyr235 and Glu233, nearly co-align at certain viewpoints along the axis pointing into the DNAs major groove. The figures were prepared using PyMOL (DeLano Scientific LLC, San Carlos, CA).

With these templates, the displacement of DNA from RNA in reactions containing RNA polymerase and ATP was enhanced by RapA (Figure 7B, lane 6). When present at quantities equimolar to that of the polymerase, of all the transcription factors that were tested, RapA was the only protein that could assist RNA polymerase in disrupting DNA–RNA complexes of this type (Figure 7B). This RapA activity required the presence of ATP (Figure 7B, lane 6, compare red and blue bars). Furthermore, increasing the RapA/RNA polymerase

molar ratio to 8:1 resulted in an increase in the amount of DNA displaced into the 'soluble' phase (Figure 7C), thus supporting the proposition that the ATP-dependent disruption of DNA–RNA complexes was mediated by RapA. In the presence of excess RapA, RNA polymerase and ATP, more than 50% of the total amount of DNA in the sample was displaced from Poly(rA)–agarose after 30 min. Furthermore, both RNA polymerase and RapA failed to disrupt these dA–dT homoduplex DNA–Poly(rA)–agarose complexes efficiently when tested
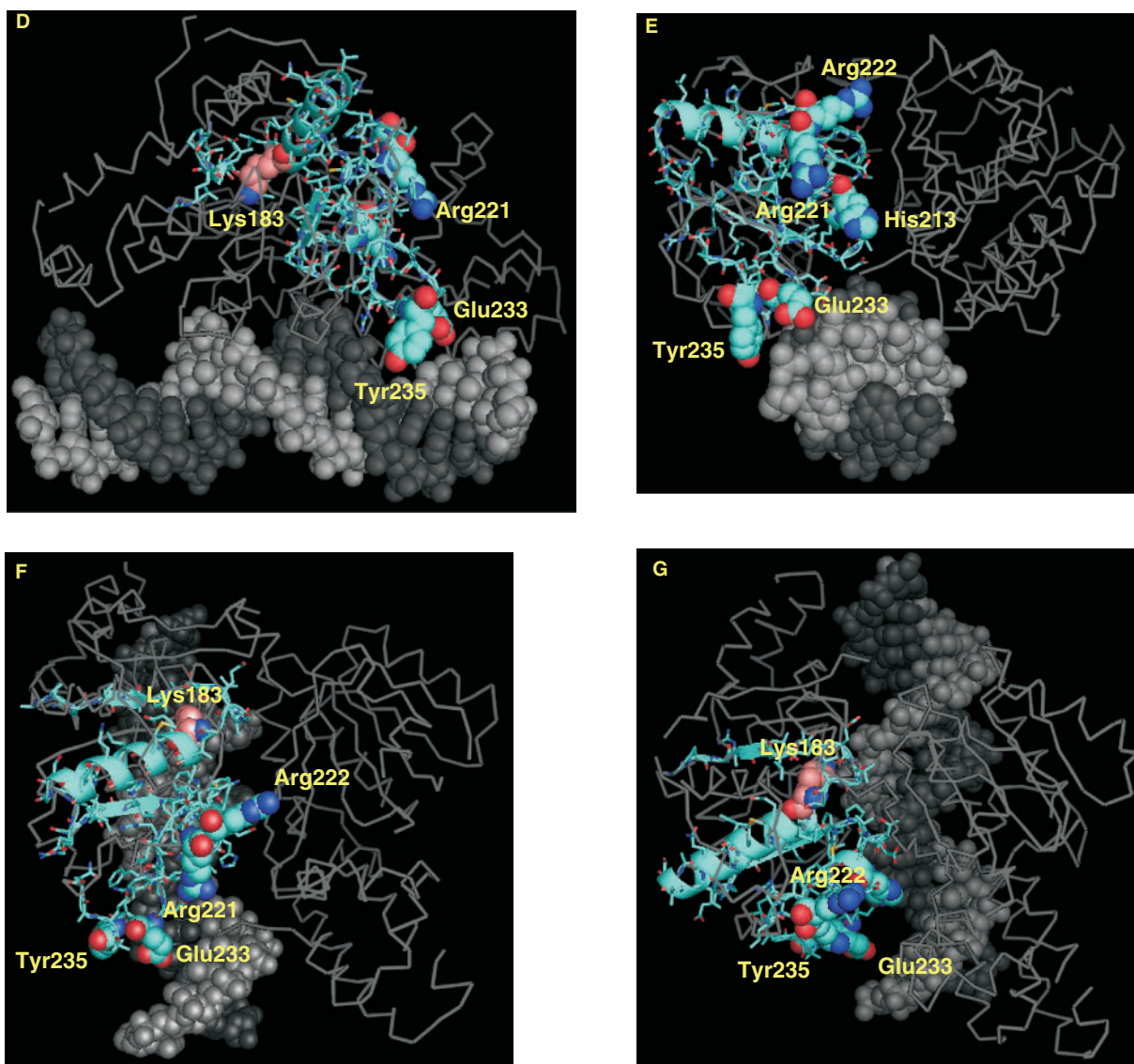
Figure 8. Continued.

separately (Figure 7C). The ability to separate RNA from DNA efficiently was gained only after mixing the two purified enzymes together (Figure 7C), further indicating the unlikelihood of contaminating enzymatic activities contributing to the observed effect. Our additional, control experiments showed that, if treated with Ribonuclease H (8 U/μl), these dA–dT homoduplex DNA–Poly(rA)–agarose complexes yielded little or no DNA in the soluble phase (data not shown), suggesting non-Watson–Crick base pairing between DNA and RNA, in accord with our PAGE-based study of similar DNA–RNA complexes.

DISCUSSION

The nature of the explicit nucleic acid or protein substrate specificity of RapA may be the key to understanding the primary function of this protein and its

prokaryotic homologs, with possible ramifications for all SWI/SNF proteins. Existing studies associate the activity of SWI/SNF proteins almost exclusively with the remodeling of DNA and histone–DNA complexes, and the recently reported structure of the catalytic domain of the RapA homolog from *S. solfataricus* (SsoRad54) complexed to DNA (24) supports the idea of DNA binding by a bacterial SWI/SNF protein. In order to determine potential DNA-binding site(s) in RapA, we threaded RapAs amino acid sequence into the SsoRad54-DNA structure via the SWISS-MODEL Protein Modeling Server (32–34). A partial RapA sequence located within the RapA domain which includes SWI/SNF homology motifs I–III had a sequence similarity sufficient to yield a homology model of the RapA NTPase/(putative) DNA-binding module (Figure 8). The RapA and SsoRad54 sequence alignments of this homologous segment—which loosely overlaps with SWI/SNF subdomain 'I' and

includes a highly conserved lysine residue [Lys183, alanine substitution of which results in a near-knockout of the RapA ATPase activity (23)] is shown in Figure 8A. Interestingly, key differences between this partial RapA structure and that of SsoRad54 included several charged amino acids, which nearly co-align at certain viewpoints (Figure 8F and G) along the axis pointing into the DNAs major groove. Most prominent of these differences are Tyr235 and Glu233, both amino acids facing the DNAs major groove (Figure 8B, E–G). Other changes, such as Arg223 and Arg224, as well as His213, would likely fall into the interface between the two major domains of RapA [Figure 8E; even though the sequence similarity between RapA and SsoRad54 within the domain-harboring SWI/SNF homology modules V–VI was not sufficient to yield a predicted protein structure, it seems likely that the overall modular organization of the two proteins must be similar, as there is a consensus regarding the presence of SWI/SNF homology motifs V and VI in RapA (1–3) despite the noted dissimilarity of RapA to the other members of Snf2 family between helicase motifs III and V (35)].

The homology model of the putative DNA-binding domain in RapA—taken together with previously reported results indicating modulation of RapAs transcription-stimulatory activity by supercoiled-to-linear DNA template transitions (23)—further supports the idea that RapA indeed possesses an NTPase/DNA-binding or 'translocase' module. And yet, multiple, independent lines of evidence—accumulated over a decade through our studies with RapA—point to RNA as a key nucleic acid substrate of RapA. Below, we summarize these lines of evidence.

(i) Perhaps the most significant result of this study, the identification of stable RapA–RNA transcription intermediates (which was made possible by the development of specialized assays, in which non-denatured *in vitro* transcription reactions are fractionated on high-resolution (43 cm–long) 6% polyacrylamide gels containing 6 M urea) clearly points to a transient RapA-transcript interaction. The RapA–RNA complexes in question are almost certainly catalytic intermediates; their poorly defined gel mobilities are likely due to conformational heterogeneity of the RNA component. Furthermore, our study of RapAs RNA-binding affinity in a purified system also showed significantly increased RNA-binding activity of the polymerase–RapA complex compared to that of the polymerase alone. RapA showed low RNA-binding activity in conventional binding assays [Figure 2; also see (19)] yet formed RNA adducts in 'functional' *in vitro* transcription reactions. We believe that this apparent discrepancy may be due to the transient nature of the (high affinity) RapA–nucleic acid interaction, which, functionally, may serve the purpose of minimizing RapA–DNA interaction in the translocating core RNA polymerase–RapA complex. It is possible to speculate that a conformational change imposed upon RapA in termination/post-termination transcription complexes may trigger the formation of high-affinity RapA–transcript complexes and their subsequent dissociation from RNA polymerase; consistent with this, the experiments described in Figure 6 (conducted under non-denaturing conditions) point to the dissociation of RapA from steady-state transcription complexes.

(ii) Our recent, independent study indicated that potentially non-productive interactions by nascent RNA may represent a primary obstacle to continuous transcriptional cycling *in vitro* (26). In that study, we demonstrated that the transcription-stimulatory activity of RapA, under certain conditions, can be mimicked by the ribosomal protein S1 (26), an RNA-binding protein entirely composed of six loosely homologous RNA-binding modules. The obvious conclusion is that the two proteins may promote transcriptional cycling by a similar mechanism which involves protein–nascent RNA interaction (26).

(iii) Studies utilizing two independent techniques supported the formation of non-canonical DNA–RNA complexes (putative DNA–RNA triplexes) *in vitro*. These DNA–RNA complexes, which may resemble 'Hoogsteen' complexes except for their substitution of a single RNA strand for one of the DNA strands, were stabilized by relatively high salt concentrations and magnesium, consistent with previous reports (29). It is important to note that our data show formation of stable non-canonical DNA–RNA complexes well within the range of intracellular *E. coli* osmolarity [(36–38), reviewed in Ref. (39)] suggesting that these potentially non-productive DNA–RNA interactions may be relevant *in vivo*. *In vitro*, RapA promoted the RNA polymerase-mediated disruption of DNA–RNA complexes in an ATP-dependent fashion. It is tempting to speculate that these immobilized templates could mimic 'non-productive' post-termination complexes referred to earlier (23), however more detailed studies are needed to consider the possible functional significance of this novel activity of RapA. Coincidentally, a recent study with eukaryotic SWI/SNF proteins has suggested similar roles in DNA triplex remodeling (18).

(iv) A number of previously obtained results also provide correlative data pointing toward the involvement of RapA in RNA management. (a) Cross-linking of RapA at the interface of the RNA polymerase alpha and beta-prime subunits (22) and the competition for binding to the polymerase between RapA and the RNA-binding protein S1 (25) (suggesting that RapA may be positioned near or at the RNA polymerase's RNA channel), plus (b) identification of RapA as an integral element of the bacterial apparatus for RNA synthesis (19–23) also indirectly support its role in RNA management.

Taken together, arguments (i)–(iv) provide a strong basis for the role of RapA in transcript management. If RapA indeed possesses a DNA binding or 'translocase' module—as further supported by our homology modeling data—this RNA-binding activity is more likely to be in addition to its DNA-binding activity. Our work presents conclusive evidence of RapA-mediated RNA remodeling. Besides the data supporting a transient RapA–RNA interaction (which suggests a conformational change in RNA), two independent, dissimilar sets of experiments clearly indicate more substantial RapA-mediated RNA remodeling: (a) RapA made 5′-termini of RNA transcripts more accessible to T4 PNK exchange reaction (at minimum, suggesting possible peeling of the transcripts'
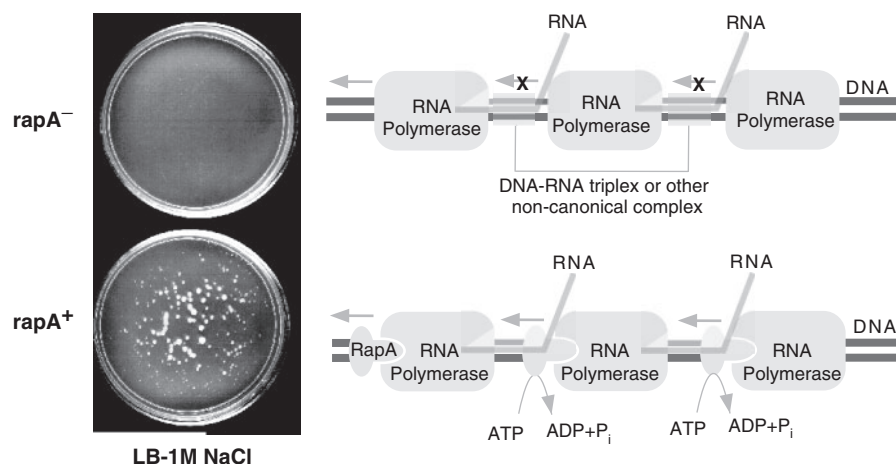
Figure 9. A model for the hypothetical function of RapA: the disruption of non-canonical DNA–RNA complexes in transcription. See text for a detailed discussion of this model.

5′-termini from either DNA or RNA polymerase), and—in agreement with this—(b) RapA promoted destabilization of non-canonical DNA–RNA complexes (putative DNA–RNA triplexes) in a system with immobilized nucleic acid templates. Both results indicate that RapA may act to free RNA transcript from non-productive interactions with either DNA or RNA polymerase. Furthermore, (c) *in vitro* transcription experiments (Figure 5B, bottom panel) also suggest such a possibility.

Taken together, our results are consistent with RapA mediating RNA release from transcription complexes (Model 1 and variant of Model 3); identification of stable RapA–RNA intermediates in functional *in vitro* transcription assays strongly supports this conclusion. Furthermore, the destabilizing effect of RapA on non-canonical DNA–RNA complexes (a variant of Model 3) also supports the RNA release model, if non-canonical DNA–RNA complexes indeed contribute to the formation of non-productive PTC. At present, we do not have any evidence in support of Model 2.

In summary, we propose that RapA remodels RNA–DNA and/or RNA–RNA polymerase complexes during transcription; this remodeling may ultimately contribute to transcript release. Our previously proposed, general model for RapA catalysis [(23); Figure 8 therein] thus remains correct; however, we have shifted emphasis from the possible destabilization of RNA polymerase–DNA complexes to remodeling of RNA–RNA polymerase and RNA–DNA complexes. We also propose that this hypothetical role of RapA in RNA remodeling may include the disruption of salt-stabilized non-canonical DNA–RNA complexes (putative DNA–RNA triplexes) (Figure 9); this activity likely accounts for pronounced slow-growth phenotype of the *rapA* deletion mutant (Figure 9, left panels; also, ref. 23), thus explaining the salt-selectivity of the *in vitro* and *in vivo* data.

ACKNOWLEDGEMENTS

Conflict of interest statement. None declared.

REFERENCES

1. Bork,P. and Koonin,E.V. (1993) An expanding family of helicases within the DEAD/H superfamily. *Nucleic Acids Res.*, **21**, 751–752.
2. Kolsto,A.B., Bork,P., Kvaloy,K., Lindback,T., Gronstadt,A., Kristensen,T. and Sander,C. (1995) Prokaryotic members of a new family of putative helicases with similarity to transcription activator SNF2. *J. Mol. Biol.*, **230**, 684–688.
3. Eisen,J.A., Sweder,K.S. and Hanawalt,P.C. (1995) Evolution of the SNF2 family of proteins: subfamilies with distinct sequences and functions. *Nucleic Acids Res.*, **23**, 2715–2723.
4. Versteege,I., Sevenet,N., Lange,J., Rousseau-Merck,M.F., Ambros,P., Handgretinger,R., Aurias,A. and Delattre,O. (1998) Truncating mutations of *hSNF5/INI1* in aggressive pediatric cancer. *Nature*, **394**, 203–206.
5. Sevenet,N., Lellouch-Tubiana,A., Schofield,D., Hoang-Xuan,K., Gessler,M., Birnbaum,D., Jeanpierre,C., Jouvet,A. and Delattre,O. (1999) Spectrum of hSNF5/INI1 somatic mutations in human cancer and genotype–phenotype correlations. *Hum. Mol. Genet.*, **8**, 2359–2368.

6. Grand,F., Kulkarni,S., Chase,A., Goldman,J.M., Gordon,M. and Cross,N.C.P. (1999) Frequent deletion of *hSNF5/INI1*, a component of the SWI/SNF complex, in chronic myeloid leukemia. *Cancer Res.*, **59**, 3870–3874.

7. Klochendler-Yeivin,A., Fiette,L., Barra,J., Muchardt,C., Babinet,C. and Yaniv,M. (2000) The murine SNF5/INI1 chromatin remodeling factor is essential for embryonic development and tumor suppression. *EMBO Rep.*, **1**, 500–506.

8. Wong,A.K.C., Shanahan,F., Chen,Y., Lian,L., Ha,P., Hendricks,K., Ghaffari,S., Iliev,D., Penn,B. *et al.* (2000) *BRG1*, a component of the SWI-SNF complex, is mutated in multiple human tumor cell lines. *Cancer Res.*, **60**, 6171–6177.

9. Guidi,C.J., Sands,A.T., Zambrowicz,B.P., Turner,T.K., Demers,D.A., Webster,W., Smith,T.W., Imbalzano,A.N. and Jones,S.N. (2001) Disruption of *INI1* leads to peri-implantation lethality and tumorigenesis in mice. *Mol. Cell. Biol.*, **21**, 3598–3603.

10. Roberts,C.M.W., Leroux,M.M., Fleming,M.D. and Orkin,S. (2002) Highly penetrant, rapid tumorigenesis through conditional inversion of the tumor suppressor gene *Snf5. Cancer Cell*, **2**, 415–425.

11. Kadonaga,J.T. (1998) Eukaryotic transcription: an interlaced network of transcription factors and chromatin-remodeling machines. *Cell*, **92**, 307–313.

12. Kingston,R.E. and Narlikar,G. (1999) ATP-dependent remodeling and acetylation as regulators of chromatin fluidity. *Genes Dev.*, **13**, 2339–2352.

13. Kornberg,R.D. and Lorch,Y. (1999) Chromatin-modifying and -remodeling complexes. *Curr. Opin. Genet. Dev.*, **9**, 148–151.

14. Struhl,K. (1999) Fundamentally different logic of gene regulation in eukaryotes and prokaryotes. *Cell*, **98**, 1–4.

15. Hamiche,A., Sandaltzopoulos,R., Gdula,D.A. and Wu,C. (1999) ATP-dependent histone octamer sliding mediated by the chromatin remodeling complex NURF. *Cell*, **97**, 833–842.

16. Langst,G., Bonte,E.J., Corona,F.V. and Becker,P.B. (1999) Nucleosome movement by CHRAC and ISWI without disruption or *trans*-displacement of the histone octamer. *Cell*, **97**, 843–852.

17. Saha,A., Wittmeyer,J. and Cairns,B.R. (2002) Chromatin remodeling by RSC involves ATP-dependent DNA translocation. *Genes Dev.*, **16**, 2120–2134.

18. Whitehouse,I., Stockdale,C., Flaus,A., Szczelkun,M.D. and Owen-Hughes,T. (2003) Evidence for DNA translocation by the ISWI chromatin-remodeling enzyme. *Mol. Cell. Biol.*, **23**, 1935–1945.

19. Sukhodolets,M.V. and Jin,D.J. (1998) RapA, a novel RNA polymerase-associated protein, is a bacterial homolog of SWI2/SNF2. *J. Biol. Chem.*, **273**, 7018–7023.

20. Muzzin,O., Campbell,E.A., Xia,L., Severinova,E., Darst,S.A. and Severinov,K. (1998) Disruption of *Escherichia coli* hepA, an RNA polymerase-associated protein, causes UV-sensitivity. *J. Biol. Chem.*, **273**, 15157–15161.

21. Sukhodolets,M.V., Garges,S. and Jin,D.J. (2003) Purification and activity assays of RapA, the RNA polymerase-associated homolog of the SWI/SNF superfamily. *Meth. Enzymol.*, **370**, 283–290.

22. Sukhodolets,M.V. and Jin,D.J. (2000) Interaction between RNA polymerase and RapA, a bacterial homolog of SWI2/SNF2. *J. Biol. Chem.*, **275**, 22090–22097.

23. Sukhodolets,M.V., Cabrera,J.E., Zhi,H. and Jin,D.J. (2001) RapA, a bacterial homolog of SWI2/SNF2, stimulates RNA polymerase recycling in transcription. *Genes Dev.*, **15**, 3300–3341.

24. Durr,H., Korner,C., Muller,M., Hickman,V. and Hopfner,K.-P. (2005) X-Ray structure of the *Sulfolobus solfataricus* SWI2/SNF2 ATPase core and its complex with DNA. *Cell*, **121**, 363–373.

25. Sukhodolets,M.V. and Garges,S. (2003) Interaction of *Escherichia coli* RNA polymerase with the ribosomal protein S1 and the Sm-like ATPase Hfq. *Biochemistry*, **42**, 8022–8034.

26. Sukhodolets,M.V., Garges,S. and Adhya,S. (2006) Ribosomal protein S1 promotes transcriptional cycling. *RNA*, **12**, 1505–1513.

27. Reynolds,R., Bermudez-Cruz,R.M. and Chamberlin,M.J. (1992) Parameters affecting transcription termination by *Escherichia coli* RNA polymerase. *J. Mol. Biol.*, **224**, 31–51.

28. Roberts,R.W. and Crothers,D.M. (1992) Stability and properties of double and triple helices: dramatic effects of RNA or DNA backbone composition. *Science*, **258**, 1463–1466.

29. Morvan,F., Imbach,J.L. and Rayner,B. (1997) Comparative stability of eight triple helices formed by differently modified DNA or RNA pyrimidine strands and a DNA hairpin. *Antisense Nucleic Acid Drug Dev.*, **7**, 327–334.

30. Ivanov,S., Alekseev,Y., Bertrand,J.R., Malvy,C. and Gottikh,M.B. (2003) Formation of stable triplexes between purine RNA and pyrimidine oligodeoxyxylonucleotides. *Nucleic Acids Res.*, **31**, 4256–4263.

31. Uptain,S.M. and Chamberlin,M.J. (1997) *Escherichia coli* RNA polymerase terminates transcription efficiently at rho-independent terminators on single-stranded DNA templates. *Proc. Natl Acad. Sci. USA*, **94**, 13548–13553.

32. Peitsch,M.C. (1995) Protein modeling by E-mail. *Bio/Technology*, **13**, 658–660.

33. Guex,N. and Peitsch,M.C. (1997) SWISS-MODEL and the Swiss-PdbViewer: an environment for comparative protein modeling. *Electrophoresis*, **18**, 2714–2723.

34. Schwede,T., Kopp,J., Guex,N. and Peitsch,M.C. (2003) SWISS-MODEL: an automated protein homology-modeling server. *Nucleic Acids Res.*, **31**, 3381–3385.

35. Flaus,A., Martin,D.M., Barton,G.J. and Owen-Huighes,T. (2006) Identification of multiple distinct Snf2 subfamilies with conserved structural motifs. *Nucleic Acids Res.*, **34**, 2887–2905.

36. Cayley,S., Lewis,B.A., Guttman,H.J. and Record,M.T.Jr (1991) Characterization of the cytoplasm of *Escherichia coli* K-12 as a function of external osmolarity. *J. Mol. Biol.*, **222**, 281–300.

37. Cayley,S. and Record,M.T.Jr (2003) Roles of cytoplasmic osmolytes, water, and crowding in the response of *Escherichia coli* to osmotic stress: biophysical basis of osmoprotection by glycine betaine. *Biochemistry*, **42**, 12596–12609.

38. Cayley,S. and Record,M.T.Jr (2004) Large changes in cytoplasmic biopolymer concentration with osmolality indicate that macromolecular crowding may regulate protein–DNA interactions and growth rate in osmotically stressed *Escherichia coli* K-12. *J. Mol. Recognit.*, **17**, 488–496.

39. Record,M.T.Jr, Courtenay,E.S., Cayley,S. and Guttman,H. (1998) Biophysical compensation mechanisms buffering *E. coli* protein–nucleic acid interactions against changing environments. *Trends Biochem. Sci.*, **23**, 190–194.